Preparation, structural and photoluminescent properties of CdS/silicon nanoporous pillar array

2007 J. Phys.: Condens. Matter 19 056003

(http://iopscience.iop.org/0953-8984/19/5/056003)

INSTITUTE OF PHYSICS PUBLISHING JOURNAL OF PHYSICS: CONDENSED MATTER

J. Phys.: Condens. Matter **19** (2007) 056003 (8pp) doi:10.1088/0953-8984/19/5/056003

Preparation, structural and photoluminescent properties of CdS/silicon nanoporous pillar array

Hai Jun Xu and Xin Jian Li

Department of Physics and Laboratory of Material Physics, Zhengzhou University, Zhengzhou 450052, People's Republic of China

Received 1 August 2006, in final form 7 December 2006
Published 15 January 2007
Online at stacks.iop.org/JPhysCM/19/056003

Abstract

A silicon nanoporous pillar array (Si-NPA) is a silicon hierarchical structure with regularly patterned surface morphology. Through a heterogeneous reaction process, nanocrystallites of cadmium sulfide (nc-CdS) were grown onto Si-NPA and a uniquely patterned nanocomposite structure (CdS/Si-NPA) was obtained. The nc-CdS, whose average size was evaluated to be ∼25 nm, mainly grew at two typical sites of the Si-NPA. One was the top sites of the porous pillars where nc-CdS clusters were formed, and the other was the valley sites surrounding the porous pillars where nc-CdS rings were formed. The nc-CdS was proved to be separated from the Si-NPA substrate by a thin layer of SiO_2 with a thickness of ∼1.3 nm. In addition to the two red photoluminescence (PL) bands observed in the Si-NPA, a green PL band peaked at ∼495 nm was observed in CdS/Si-NPA when it was excited by 370 nm wavelength ultraviolet light. Based on these experimental results, the green and red PL bands of CdS/Si-NPA were attributed to the radiative recombination of the excitons occurring in nc-CdS and Si-NPA separately.

1. Introduction

Soon after the demonstration of strong photoluminescence (PL) in nanostructured porous silicon [1], much effort has been devoted to elaborate silicon-based nanocomposite structures [2–8], either to realize multi-band emissions or to improve the PL stability and efficiency of the substrates. For example, copper [9], diamond [10], fullerene [11], $Pb(Zr_x, Ti_{1-x})O_3$ (PZT) [12], ZnSe [13], ZnS [14, 15], ZnO [16, 17], CdSe [18] and CdS [19–22] have been used as components to fabricate silicon-based nanocomposite structures, and unique optical properties have been achieved in these systems. As one of the promising II–VI compound semiconductors, cadmium sulfide (CdS) has been found to possess the properties of high electrical conductibility, broad-spectrum light transparency and high chemical stability [23–28], and has been much considered for potential applications in the fields of solar cells [23], optoelectronics [24–26] and microelectronics [27]. In recent

years, research on CdS/Si nanocomposite structures has attracted much attention, and various preparation techniques such as the dip coating method [19], liquid–liquid interface reaction technique (LLIRT) [20, 21] and electrochemical deposition method [22] have been developed. All this research indicated that the characteristics of the silicon substrate play an important role in deciding both the microstructure and the physical properties of the targeted nanocomposite structure. Previously, we have presented the preparation and characterization of a silicon nanoporous pillar array (Si-NPA), and have predicted that its regularly patterned hierarchical structure [29, 30] might be suitable for assembling novel silicon-based nanocomposite structures. In this paper, we report that a novel CdS/Si nanocomposite structure was prepared via a heterogeneous reaction process utilizing Si-NPA as a substrate. In addition to the characterization of the surface morphology, microstructure and chemical constitution, the PL properties of CdS/Si-NPA were studied comparatively with those of Si-NPA and the related emission processes were analysed. Our results indicate that Si-NPA is an ideal template for synthesizing patterned, silicon-based nanocomposite structures with unique optical properties.

2. Experimental details

The Si-NPA substrate used here was prepared by hydrothermally etching p-type, (111) oriented single-crystal silicon wafers in a solution of hydrofluoric acid containing ferric nitrate [29]. The resistivity of the initial silicon wafers was 0.015 Ω cm. After hydrothermal etching, special washing and drying procedures were adopted to avoid the possible structural damage which might be caused by surface stress. The nanophased CdS particles were grown onto Si-NPA by a heterogeneous reaction process at room temperature. The Si-NPA substrates were first immersed in an aqueous solution of 0.01 mol l^{-1} $CdCl_2$ for 20 h and then dried by nitrogen blowing. Then the as-immersed Si-NPA was exposed to a flux of H_2S for 20 h to guarantee that all the adsorbed $CdCl_2$ reacts with H_2S completely. The formation process of CdS could be described simply by the following chemical reaction formula: $CdCl_2$ (s) + H_2S (g) = CdS (s) + 2HCl (g). Lastly, a rapid thermal annealing process was carried out at 300 °C in N_2 atmosphere, aiming to obtain suitably crystallized CdS nanocrystallites (nc-CdS).

The determination of the surface morphology, microstructure and chemical constitution were accomplished by field-emission scanning electron microscopy (FE-SEM), energy-dispersive x-ray spectrometry (EDS), x-ray diffraction (XRD), and x-ray photoelectron spectroscopy (XPS) experiments. The PL spectra and the absorption spectrum were measured using a Hitachi F-4500 fluorescence spectrometer and Shimadzu UV-3150 spectrophotometer, respectively.

3. Results and discussion

Figure 1(a) shows the typical surface morphology of Si-NPA, the substrate adopted in the experiment. Here a regular array composed of large quantities of well-separated, quasi-identical silicon pillars is clearly observed. Just as has been described previously [29, 30], Si-NPA is a micron/nanometre structural composite system with a distinct triple hierarchical structure, i.e. an array composed of micron-sized silicon pillars, nanopores densely distributed on the pillars, and silicon nanocrystallites forming the pore walls. These structural features make Si-NPA become a possible template for assembling functional silicon-based nanocomposite systems with patterned structures.

The formation of CdS after the heterogeneous reaction process was proved by the results of the XRD experiment, which are depicted in figure 2. From the typical surface morphology of CdS/Si-NPA given in figures 1(b)–(d), it can be found that the growth of CdS on Si-NPA

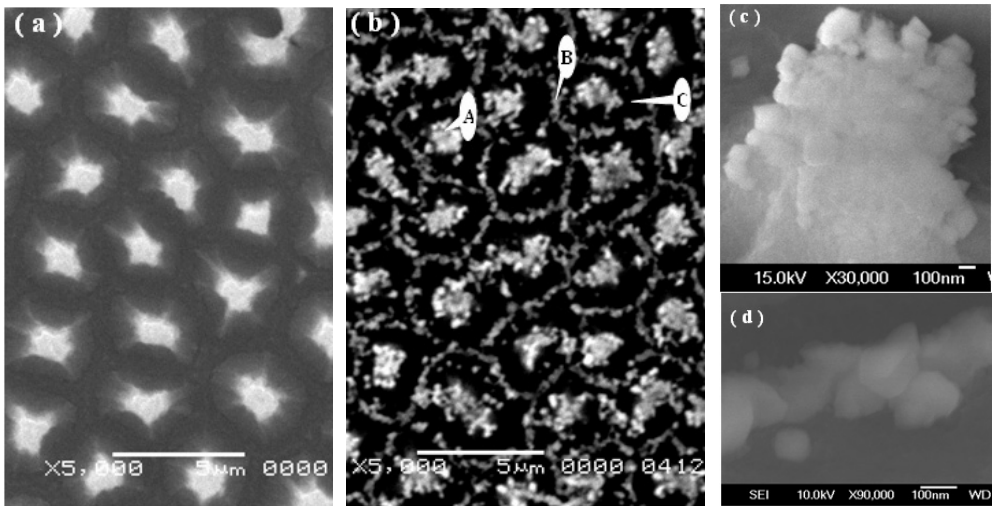

Figure 1. Typical FE-SEM micrographs of Si-NPA (a), CdS/Si-NPA nanocomposite structure (b), clusters of nc-CdS at the top site of a pillar (c), and a section of a CdS ring surrounding the pillar (d), respectively. The images presented in (c) and (d) were taken with the samples tilted at an angle of 45°. Sites marked by A, B and C in (b) indicate the typical sites selected for carrying out the EDS experiments.

was through a site-selection mode. The accumulation of nc-CdS occurred only at two typical sites on the surface of Si-NPA: the top sites of the pillars (figure 1(c)) and the valley sites surrounding the pillars (figure 1(d)). It is interesting that the nc-CdS accumulated at the latter sites formed almost well-defined CdS rings. As is known, a decrease in the grain size would definitely lead to a broadening of the corresponding XRD diffraction peak and, based on this, the average size of the nanocrystallites of a certain material could be evaluated according to Scherrer's formula [22]. Based on the experimental data corresponding to the (002) diffraction peak of CdS appearing at 26.4° (figure 2), the average size of the nc-CdS was calculated to be ∼25 nm. This value was much smaller than that of the observed particles in figures 1(c) and (d) (∼35–200 nm), which indicates that the particles observed by FE-SEM, both on the CdS rings surrounding the pillars and the clusters at the top sites of the pillars, were composed of nc-CdS with smaller sizes.

The distribution of the deposited CdS on Si-NPA was non-homogeneous (figure 1(b)). To give a qualitative description of the distribution of elements on the surface of CdS/Si-NPA, EDS measurements were carried out at three typical sites, which represented areas with different geometrical features and are indicated by A, B, and C in figure 1(b). The corresponding experimental EDS data are presented in table 1. Clearly, at the top sites of the pillars (site A), the detected atom percentages for silicon, oxygen, cadmium and sulphur were 50.62%, 41.61%, 3.41% and 4.36%, respectively; while those detected at the CdS rings surrounding the pillars (site B) were 70.14%, 23.32%, 2.90% and 3.64%, correspondingly. For sites without a trace of CdS, judged from the FE-SEM image (site C), the corresponding atom percentages were 64.37%, 34.60%, 0.41% and 0.62%. Considering the fact that the effective irradiating radius of the electron-beam spot in the present EDS experiment was ∼0.5 μm, it is reasonable to conclude that CdS mainly grows at the top sites of the pillars and the rings surrounding the pillars. This result means that the growth of CdS on Si-NPA was site-selective. Investigation of the reason for the site-selective growth of CdS on silicon is of practical importance.

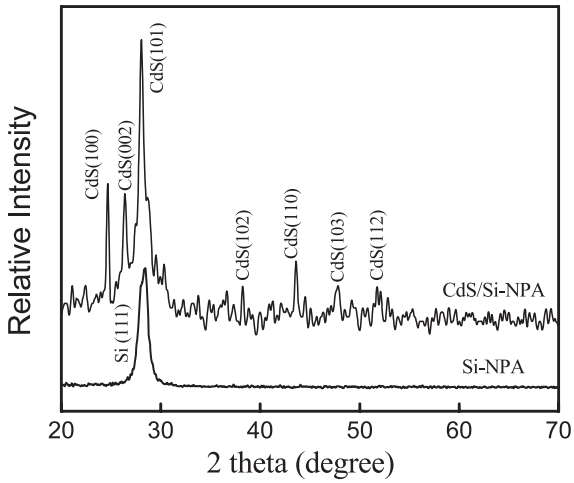

Figure 2. XRD patterns of Si-NPA substrate and CdS/Si-NPA nanocomposite structure.

Table 1. Element distribution at three typical sites on CdS/Si-NPA (Note: all results at.%).

Site	Si	O	S	Cd	Total
Site A	50.62	41.61	4.36	3.41	100.00
Site B	70.14	23.32	3.64	2.90	100.00
Site C	64.37	34.60	0.62	0.41	100.00

What should be noted especially is the high oxygen atom percentage reflected by the EDS measurements given in table 1 (41.61% at site A, 23.32% at site B, and 34.60% at site C), but such a high oxygen content was not reflected by the XRD pattern of CdS/Si-NPA. Considering the device design and function stabilization, the origin and the existing status of these oxygen atoms must be clarified. As is known from the description given above, the whole process of the chemical reaction for forming CdS is carried in a reducing atmosphere, so the oxygen content detected in CdS/Si-NPA could only originate from oxygen adsorption or the fabrication procedures before the chemical reaction. If the oxygen content is proved to exist as adsorbed atoms, it would be very harmful to device fabrication. Therefore, we carried out the XPS experiments on a Si-NPA substrate before CdS growth, and the results are presented in figure 3. Here three peaks are observed, corresponding to the binding energy of Si 2p, Si 2s, and O 1s, respectively. Judging from the binding energy values of the peak positions given in the insets of figure 3 (i.e. ∼103 eV for the binding energy of Si 2p electrons (left) and ∼532–534 eV for the binding energy of O 1s electrons (right)), it can be concluded that the existing states of silicon and oxygen elements are in the form SiO_2 [31, 32]. This result indicates that there a thin layer of SiO_2 might have natively formed on the surface of the Si-NPA. Based on the XPS experimental data and adopting the calculation method used in [33], the layer thickness of SiO_2 was estimated to be ∼1.3 nm. From this result, it could be directly deduced that, in as-prepared CdS/Si-NPA nanocomposite structure, nc-CdS was separated from Si-NPA substrate by a SiO_2 nanolayer. Also, as a result, the electronic structure and physical properties of CdS/Si-NPA as a whole is decided by the two sub-nanosystems, nc-CdS and Si-NPA, together with their possible quantum coupling across the SiO_2 nanolayer.

In order to investigate the PL variation brought about by the newly incorporated nc-CdS, the PL spectra of both Si-NPA and CdS/Si-NPA were measured at room temperature, and the

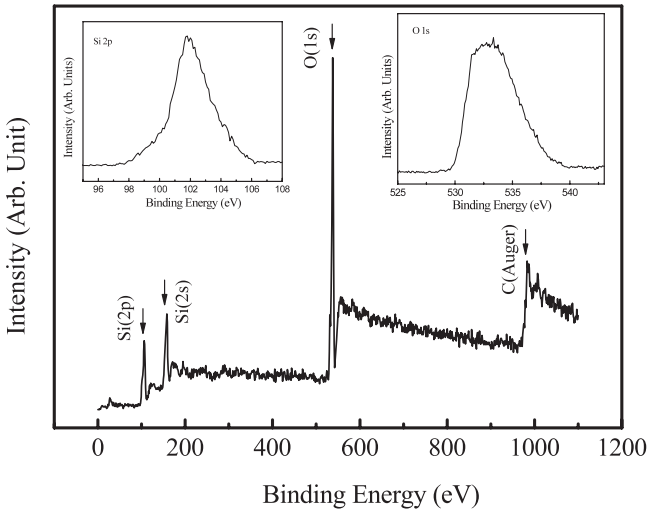

Figure 3. XPS spectra of Si-NPA. Left inset: fine spectrum for Si 2p peak. Right inset: fine spectrum for O 1s peak.

results are presented in figure 4. Clearly, under excitation by 370 nm ultraviolet light, both the strength and the shape profile of the PL spectrum of CdS/Si-NPA changed tremendously compared with that of Si-NPA. By adopting the multi-peak Gaussian fitting method, the experimentally obtained PL spectra of Si-NPA and CdS/Si-NPA could be decomposed as two emission bands and three emission bands, respectively. The two PL peaks of Si-NPA are located at ∼715 nm and ∼630 nm, and the three PL peaks of CdS/Si-NPA are located at ∼718 nm, ∼635 nm, and ∼495 nm. Comparing the red PL bands from both Si-NPA and CdS/Si-NPA, it is easy to find that the difference between the corresponding peak positions are very small, 3 and 5 nm respectively, and the full width at half maximum (FWHM) of the corresponding peaks are also almost the same. Based on these experimental data, it is reasonable to deduce that the two red PL bands of CdS/Si-NPA should be directly related to the emission from Si-NPA and, most probably, they might have the same emission process.

The green emission band peaked at ∼495 nm in the PL spectrum of CdS/Si-NPA was the most notable difference from that of Si-NPA, and it can be directly related to the nc-CdS in the nanocomposite structure. According to results of the studies on CdS/Si nanocomposites by other groups [34–36], a novel emission band, which was different from that of silicon substrate and peaked at 420–500 nm, would be observed and has been due to the intrinsic radiative recombination of excitons in nc-CdS. It was also demonstrated that when the size of nc-CdS approached 50 nm, the corresponding PL peak energy approaches the band-gap energy of bulk CdS, ∼512 nm (2.42 eV), because of the gradual weakening and final disappearance of the exciton confinement [34]. Therefore, the emission band peaked at ∼495 nm (2.51 eV) (figure 4) should originate from the intrinsic radiative recombination of excitons in the nc-CdS of CdS/Si-NPA. Compared with that of bulk CdS, the PL peak energy of CdS/S-NPA exhibits a blue-shift of ∼0.09 eV (17 nm). The blue-shift should come from the quantum confinement effect of the excitons in nc-CdS, because the average size (∼25 nm) of nc-CdS estimated above is much smaller than 50 nm, which is the size suggested for observing an eminent blue-shift of the PL peak energy [34]. This inference can be further confirmed from the result of the light absorption experiment on CdS/Si-NPA carried out at room temperature (the inset of figure 4). Here an absorption peak located at ∼490 nm (2.53 eV) is observed. This value (2.53 eV) is

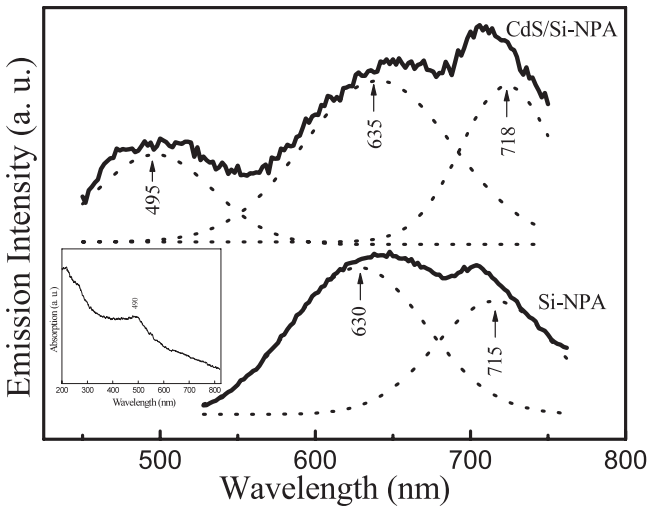

Figure 4. Room-temperature PL spectra of CdS/Si-NPA and Si-NPA excited by 370 nm ultraviolet radiation (solid lines) and fitting curves (dotted lines). Inset: absorption spectrum of CdS/Si-NPA.

much larger than the band gap of bulk CdS (∼2.42 eV) and very close to the observed PL peak energy of CdS/Si-NPA (∼2.51 eV) of the green band.

The evolution of the three PL bands of CdS/Si-NPA with excitation wavelength was studied by varying the wavelength from 340 to 430 nm, with a step of 30 nm, and the results are depicted in figure 5. It can be found that the intensity of all three emission bands decreases with excitation wavelength, but the peak position of the green band evolves differently from those of the two red PL bands. As the excitation wavelength was chosen to be 340, 370, 400 and 430 nm, the corresponding peak positions of the green bands, which were determined by the multi-peak Gaussian fitting method, were ∼490, ∼495, ∼498 and ∼500 nm respectively, as is given in the inset of figure 5. This indicates that the peak energy of the green PL band of CdS/Si-NPA depends strongly upon the excitation wavelength: the shorter the excitation wavelength employed, the higher the peak energy obtained. This evolution behaviour of the PL peak energy with excitation wavelength has been generally accepted as an indication of exciton quantum confinement in semiconductor nanomaterials. On the other hand, no blue-shift of the peak energy was found for the two red PL bands. Therefore, it can be concluded that in as-prepared CdS/Si-NPA nanocomposite structure, the green PL and red PL originate from the radiative recombination of excitations in nc-CdS and Si-NPA, respectively. As for the understanding of the PL excitation process of CdS/Si-NPA, and especially the clarification of whether there is quantum tunnelling of excited electrons from nc-CdS to Si-NPA across the SiO_2 nanolayer, further in-depth research is needed.

4. Conclusion

Utilizing regularly patterned and hierarchically structured Si-NPA as substrate, a novel CdS/Si nanocomposite structure was prepared by depositing nc-CdS through a simple heterogeneous reaction process. It is disclosed that the growth of CdS on Si-NPA was site-selective and finally led to the formation of a uniquely patterned structure. In CdS/Si-NPA, a green PL band newly appeared, in addition to the two red PL bands observed in Si-NPA. Analysis of the spectral measurements indicated that, in the PL emission process of CdS/Si-NPA, the green emission

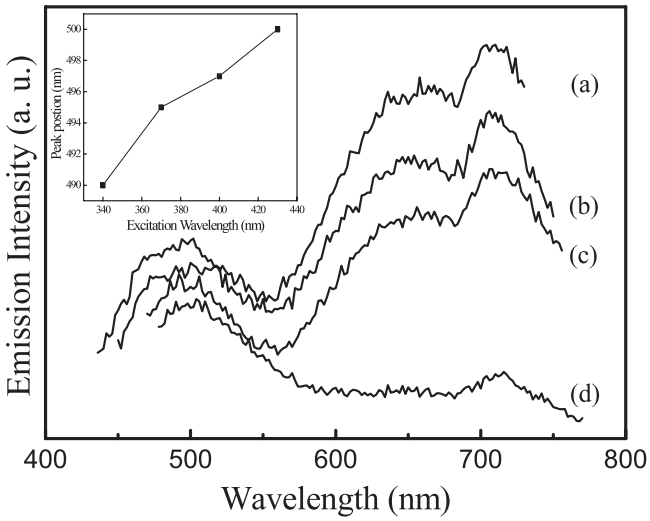

Figure 5. Room-temperature PL spectra of CdS/Si-NPA excited by (a) 340 nm, (b) 370 nm, (c) 400 nm, and (d) 430 nm wavelengths, respectively. Inset: evolution of peak position of green PL band with excitation wavelength.

occurs in nc-CdS and the red emissions come from Si-NPA. Much research is needed to clarify the mechanism of the PL excitation process and the possible quantum tunnelling of excited electrons between nc-CdS and Si-NPA across the SiO_2 nanolayer.

Acknowledgment

This project is supported by National Natural Science Foundation of China (NSFC, no. 10574112).

References

[1] Canham L T 1990 *Appl. Phys. Lett.* **57** 1046–8
[2] Fan S, Chapline M G, Franklin N R, Tombler T W, Cassell A M and Dai H J 1999 *Science* **283** 512–4
[3] Jole J L and Wang Z L 2001 *Nano Lett.* **8** 449–51
[4] Martin E, Torres-Costa V, Martin-Palma R J, Bousono C, Tutor-Sanchez J and Martinez-Duart J M 2006 *J. Electrochem. Soc.* **153** D134–7
[5] Oton C J, Navarro-Urrios D, Capuj N E, Ghulinyan M, Pavesi L, Gonzalez-Perez S, Lahoz F and Martin I R 2006 *Appl. Phys. Lett.* **89** 011107
[6] Chan S, Kwon S, Koo T W, Lee L P and Berlin A A 2003 *Adv. Mater.* **15** 1595–8
[7] Wang S, Choi D G and Yang S M 2002 *Adv. Mater.* **14** 1311–4
[8] Yu K, Zhang Y, Xu R, Jiang D, Luo L, Li Q, Zhu Z and Lu W 2005 *Solid State Commun.* **133** 43–7
[9] Ghosh S, Hong K and Lee C 2002 *Mater. Sci. Eng.* B **96** 53–9
[10] Baranauskas V, Li B B, Peterlevitz A C, Tosin M C and Durrant S F 1999 *Thin Solid Films* **355/356** 233–8
[11] Wu X L, Deng Z H, Xue F S, Siu G G and Chu P K 2006 *J. Chem. Phys.* **124** 214706
[12] Chen Q W, Zhu D L, Zhu C, Wang J and Zhang Y G 2003 *Appl. Phys. Lett.* **82** 1018–20
[13] Li Q, Hark S K, Wang J, Xu Y M, Wang C R and Lau W M 2005 *Appl. Phys. Lett.* **87** 211917
[14] Cheah K W, Xu L and Huang X 2002 *Nanotechnology* **13** 238–42
[15] Xu L, Cheah K W, Tam H L, Li K F, Zhang Y, Ma Y, Hang X and Chen K 2002 *Japan. J. Appl. Phys.* **41** 4466–8
[16] Li Y, Feneberg M, Reiser A, Schirra M, Enchelmaier R, Ladenburger A, Langlois A, Sauer R, Thonke K, Cai J and Rauscher H 2006 *J. Appl. Phys.* **99** 054307

[17] Hsu H C, Cheng C S, Chang C C, Yang S, Chang C S and Hsieh W F 2005 *Nanotechnology* **16** 297–301
[18] Belogorokhov A I, Belogorokhova L I, Perez-Rodriguez A, Morante J R and Gavrilov S 1998 *Appl. Phys. Lett.* **73** 2766–8
[19] Deshmukh N V, Bhave T M, Ethiraj A S, Sainkar S R, Ganesan V, Bhoraskar S V and Kulkarni S K 2001 *Nanotechnology* **12** 290–4
[20] Gokarna A, Pavaskar N R, Sathaye S D, Ganesan V and Bhoraskar S V 2002 *J. Appl. Phys.* **92** 2118–24
[21] Gokarna A, Bhoraskar S V, Pavaskar N R and Sathaye S D 2000 *Phys. Status Solidi* a **182** 175–9
[22] Zhang P, Kim P S and Sham T K 2002 *J. Appl. Phys.* **91** 6038–43
[23] Dobson K D, Visoly-Fisher I, Hodes G and Cahen D 2001 *Adv. Mater.* **13** 1495–9
[24] Prabhakaran K, Meneau F, Sankar G, Sumitomo K, Murashita T, Homma Y, Greaves G N and Ogino T 2003 *Adv. Mater.* **15** 1522–6
[25] Greytak A B, Barrelet C J, Li Y and Lieber C M 2005 *Appl. Phys. Lett.* **87** 151103
[26] Agarwal R, Barrelet C J and Lieber C M 2005 *Nano Lett.* **5** 917–20
[27] Duan X, Huang Y, Agarwal R and Lieber C M 2003 *Nature* **421** 241–5
[28] Jun Y W, Lee S M and Cheon J 2001 *J. Am. Chem. Soc.* **123** 5150–1
[29] Li X J, Hu X, Jia Y and Zhang Y H 1999 *Appl. Phys. Lett.* **75** 2906–8
[30] Xu H J, Fu X N, Sun X R and Li X J 2005 *Acta Phys. Sin.* **54** 2352–7
[31] Chen X Y, Lu Y F, Tang L J, Wu Y H, Cho B J, Xu X J, Dong J R and Song W D 2005 *J. Appl. Lett.* **97** 014913
[32] Korsunskaya N E, Torchinskaya T V, Khomenkova L Yu, Dzhumaev B R and Prokes S M 2000 *Microelectron. Eng.* **51/52** 485–93
[33] Mitchell D F, Clark K B, Bardwell J A, Leonard W N, Massoumi G R and Mitchell I V 1994 *Surf. Interface Anal.* **21** 44–50
[34] Lei Y, Chim W K, Sun H P and Wilde G 2005 *Appl. Phys. Lett.* **86** 103106
[35] Ge J and Li Y 2004 *Adv. Funct. Mater.* **14** 157–62
[36] Liu W, Jia C, Jin C, Yao L, Cai W and Li X 2004 *J. Cryst. Growth* **269** 304–9